Oxidation of Fe–Cr–Al and Fe–Cr–Al–Y Single Crystals

H. J. Grabke, M. Siegers, and V. K. Tolpygo

Max-Planck-Institut für Eisenforschung GmbH, Max-Planck-Str. 1, 40237 Düsseldorf, Germany

Z. Naturforsch. **50a**, 217–227 (1995); received November 14, 1994

Dedicated to Prof. Dr. Dr. h.c. Dr. E.h. E. Wicke on the occasion of his 80th birthday

Single crystal samples of the alloy Fe-20%Cr-5%Al with and without Y-doping were used to study the "reactive element" (RE) effect, which causes improved oxidation behaviour and formation of a protective Al_2O_3 layer on this alloy. The oxidation was followed by AES at 10^{-7} mbar O_2 up to about 1000 °C. Most observations were peculiar for this low pO_2 environment, but yttrium clearly favors the formation of Al-oxide and stabilizes it also under these conditions, probably by favoring its nucleation. The oxides formed are surface compounds of about monolayer thickness, not clearly related to bulk oxides.

Furthermore, the morphologies of oxide scales were investigated by SEM, after oxidation at 1000 °C for 100 h at 133 mbar O_2. On Fe–Cr–Al the scale is strongly convoluted and tends to spalling, whereas the presence of Y leads to flat scales which are well adherent. This difference is explained by a change in growth mechanism. The tendency for separation of oxide and metal was highest for the samples with low energy metal surface, i.e. (100) and (110), the scale was better adherent on the (111) oriented surface and on the polycrystalline specimen, since in the latter cases the overall energy for scale/metal separation is higher.

All observations, from the low and from the high pO_2 experiments, are discussed in relation to the approximately ten mechanisms proposed in the literature for explanation of the RE effects.

Introduction

All high temperature alloys must rely on the formation of a stable, dense, slowly growing oxide scale for protection against oxidation and attack by corrosive gases and/or deposits. Generally, either Al_2O_3- or Cr_2O_3-forming alloys are used, the chromia forming alloys in a lower temperature range up to < 1100 °C since at very high temperatures volatile chromium oxides and other volatile compounds lead to loss of the scale. Fe–Cr–Al alloys are widely used at temperatures > 900 °C, e.g. for heating wires and as support for the catalyst for automotive exhaust gases. The composition usually corresponds to about Fe-20%Cr-5%Al, but a small addition of a rare earth element is necessary to obtain a well adherent, protective scale. This "rare earth element effect" has been known since more than 50 years, and has been widely used since then. The addition of some rare earth element, Ce, Y, La..., to high temperature alloys is advantageous not only for Fe–Cr–Al but also for many other alumina forming as well as chromia forming alloys. Later it was found that not only the rare earth elements but also some other reactive elements (RE) such as Ti, Zr, Hf... are helpful. The RE effects are numerous but most are positive: (i) improvement of scale adherence, (ii) support of the selective oxidation of the element, which forms the protective scale, (iii) retardation of scale growth (not always), (iv) fine grained scale with improved ductility.

The rare earth or reactive element effect has been known since long and the discussion on its reasons lasts just as long. Many theories and experimental results have been put forward and have been summarized now and then [1–5]. For some explanations, exclusive validity was claimed, but to our opinion all these explanations are more or less right and more or less well applicable in different cases.

In the following a short summary will be given of the explanations proposed as yet:

1. Heterogeneous Nucleation of Oxide

The rare earth metals are most oxygen affine metals and the very first components of an alloy to be oxidized. This yields oxide particles dispersed in the alloy surface which can act as nucleation sites for the protective oxide to be formed. Thereby, the internuclei spacings are decreased and also the time required for subsequent lateral growth to link the nuclei and form

Reprint requests to Prof. Dr. H. J. Grabke.

0932-0784 / 95 / 0200-0217 $ 06.00 © – Verlag der Zeitschrift für Naturforschung, D-72027 Tübingen

a complete layer. This mechanism is consistent with various observations, e.g. on the promotion of selective Cr_2O_3 formation [6].

2. *"Graded Seal" Layer*

The formation of an oxide or other compound containing the reactive element was assumed, as an intermediate layer, which provides a gradual transition of lattice constant and thermal expansion coefficient, such a layer should decrease the effect of thermal expansion coefficient differences. Accordingly, the oxide scale should show less propensity to spalling upon cooling and thermal cycling. Such graded-seal layer was observed on Fe–Al–Ti alloys, i.e. a layer of Ti oxycarbide [7, 8], epitaxially growing with gradually changing O/C ratio and lattice constant. This layer favors the nucleation of α-Al_2O_3 and its adherence.

3. *Modification to Growth Processes*

On an Al_2O_3 forming alloy without RE additions the generally accepted growth mechanism of α-Al_2O_3 is by simultaneous counter-current diffusion of oxygen and aluminum mainly in the grain boundaries. Thereby, the oxide is formed in the interior of the layer (Fig. 1 a, b) which leads to compressive stresses in the scale and its lateral growth. After reaching a certain layer thickness these stresses may lead to scale/substrate separation (Figure 1 b). In the case of strong oxide/metal bonding and sufficient metal plasticity the substrate is deformed with the scale (Figure 1 a). In yttrium containing Fe–Cr–Al alloys the outward diffusion of aluminum is suppressed and the oxide scale grows mainly by inward diffusion of oxygen along grain boundaries, as was proven by tracer experiments with ^{16}O and ^{18}O [9, 10]. Prevailing inward diffusion shifts the location of oxide growth to the inner phase boundary, which is considered a better place than the interior of the layer. In this case (Fig. 1 c) but also in the case of prevailing outward diffusion of cations (Fig. 1 d) the scale can stay well adherent. There are authors [11, 12] who deduce the latter growth mechanism of alumina from their tracer and marker experiments.

4. *Scavenging of Impurities*

It has been shown that the reduction of the sulfur content in high temperature alloys leads to improved

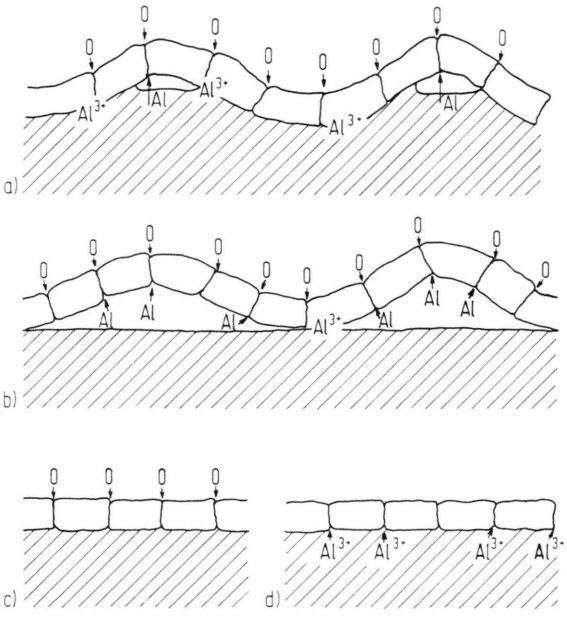

Fig. 1. Mechanisms and morphologies of alumina scale growth, a) and b) counterdiffusion of oxygen and cations, mainly at grain boundaries, leading to convoluted scale, separation of scale and metal in the case (a) only in the region of high tensile stress (b) buckling of the scale and nearly complete separation, e.g. for low energy metal surface orientations, c) and d) diffusion only in one direction, as effected by RE, and leading to plane scales with good adherence.

adherence of the scale [13–17]. This "sulfur effect" had been explained by sulfur segregation to the oxide/metal interface causing loss of cohesion. However, such segregation is highly improbable [18, 19] and it has been clarified that the sulfur segregates to the free metal surface of separations and cavities, immediately upon their formation. This process causes a decrease of surface energy of the nascent metal surface and favors the separation resp. cavity formation. In the case of the Fe–Cr–Al alloys, presence of sulfur in cavities was demonstrated by AES, in the intact interface the sulfur concentration was much less [20]. But in fact, the presence of sulfur favors and accelerates the separation of oxide and metal, caused by growth stresses as described (Figure 1). The role of the RE is to scavenge sulfur by formation of very stable sulfides or oxysulfides.

Some other mechanisms have been put forward for explanation of the RE effects, which are of less credibility or at least of less importance, they will be listed here only shortly:

5. Mechanical Keying or Pegging

The pegging effect is based on the observation that in alloys containing rare earth elements often growth of oxide protrusions (pegs) into the metal is observed. These pegs anchor the oxide to the metal and render good oxide adherence [21] – but they are not observed in many cases of well adherent layers, also not in this study.

6. Enhanced Scale Plasticity

If changes in the microstructure and composition of the scale by RE facilitate plastic deformation, growth stresses in the scale can be released at oxidation temperature [22] – but not the thermal stresses upon cooling.

7. Vacancy Sink Provision

RE additions can provide sites for vacancy condensation during oxidation, e.g. oxide particles, preventing or reducing void formation and consequently suppressing separation of the scale from the substrate [23–25]. This effect may apply for fast growing oxides which grow by outward diffusion of cations (FeO, CoO, NiO), but should play no role for Al_2O_3 growth on alloys.

8. Enhanced Chemical Bonding

Theoretical calculations on the basis of the molecular orbital quantum theory predict strong bonding of Al_2O_3 to Y atoms at an alloy surface [26]. This is self evident, however, there will be no Y atoms in the alloy surface since yttrium will be oxidized even earlier than aluminum. The low Y content at the oxide/metal interface for FeNiCrAlY and the lack of an improvement in adhesion with increased Y content of the alloy also indicate that the chemical bonding hypothesis is inadequate [27].

9. Reduction of Scale Growth Rate

The growth rate of Cr_2O_3 and NiO scales are reduced by the presence of RE elements, but their influence on the oxidation rate of Al_2O_3 forming alloys is little or none [28]. The reduction in growth rate may be caused by blocking of fast diffusion paths in the oxide. If the thickening rate is decreased, critical values of thickness and growth stresses are reached after longer times. But as already pointed out, there is no clear reduction in growth rate of Al_2O_3 scale by RE.

10. Blocking of Interface Oxide/Metal

This most recent theory [29, 30] assumes segregation of RE ions at the interface oxide/metal and blocking of the interfacial reaction. Thus, the entering of cations into the scale is assumed to be hindered strongly, which would result in prevailing oxide growth by anion diffusion and slower kinetics for a tightly adherent scale.

For the present study special materials were prepared, single crystals of Fe–Cr–Al and corresponding single crystals doped with Y to study the RE effect. Surface analytical methods, AES and LEED have been applied to find out if the RE already affects the very first stages of oxide formation – as yet such experiments were missing in the numerous studies on the RE effect. It was expected that especially information on the validity of mechanisms, 1. Heterogeneous nucleation of oxide and 2. "Graded seal" layer, could be gained from such a study. The single crystal specimens also were used for thermogravimetric experiments on studies on the morphology of scale formation by scanning electron microscopy (SEM), which led to conclusions on the mechanisms 3. Modification of growth processes and 4. Scavenging of impurities.

In these ways the use of single crystal materials allowed some progress in the understanding of oxide growth and of the RE effect.

Materials

The composition of the alloys investigated is given in Table 1. The single crystals were grown using the Bridgman method. Samples with the main planes parallel to the crystal faces (100), (110) and (111) were cut by spark erosion. All samples were first annealed in flowing hydrogen at 1000 °C for 100 h, this decreases the content of C and S to the values given in Table 1.

Table 1. Chemical analysis of the alloys (in wt.%).

	Cr	Al	Y	C	S
Fe–Cr–Al poly xx	23.3	4.83	–	0.0044	0.0010
Fe–Cr–Al single x	19.5	4.50	–	0.0070	0.0010
Fe–Cr–Al–Y poly xx	23.0	4.80	0.029	0.0090	0.0039
Fe–Cr–Al–Y single x	21.7	5.42	0.003	0.0041	0.0006

The samples were ground and polished to a final finish with diamond paste, then cleaned in alcohol and dried.

Initial Stages of Oxidation

The oxidation behaviour of Fe–Cr–Al single crystal samples was observed by AES during heating to about 1000 °C under simultaneous oxidation at 10^{-7} mbar O_2 [31–33]. During the oxidation the Auger spectra were taken repeatedly in the range from 20 eV to 70 eV, where one can derive from the peak energies if the elements are present as metal in the alloy or in an oxidized state. Before and after each oxidation experiment, the complete spectrum was taken up to 800 eV (Figs. 2 and 3).

The important peaks in the low energy range are

metals	Cr 36 eV	Fe 47 eV	Al 68 eV
oxides	Cr_{ox} 32 eV	Fe_{ox} 44 eV	Al_{ox} 55 eV (and a shoulder at 40 eV).

Thus, the low energy spectrum clearly shows which alloying element is oxidized in dependence on time and temperature.

The surface structure was investigated on samples cooled after oxidation. It must be noted that in order to observe a LEED pattern the samples had to be annealed before oxidation (in UHV) and this caused an enrichment of Al by segregation to the surface.

Fe–Cr–Al

The single crystal samples with different orientations (110), (100) and (111) showed similar oxidation behaviour in the AES investigation. During heating of the specimens at first, at about 500 °C, spinels started to grow as can be derived from the appearance of the oxygen peak and the increase of the Cr peak. Upon further temperature increase the Al-peak increases and the peak for oxidized Al appears in the low energy range and grows, see Fig. 2a, simultaneously the Cr peak decreases. Obviously, the spinel is reduced by Al under formation of aluminum oxide at the surface. These observations are well in agreement with what was to be expected according to the experience at normal pressure. However, at higher temperature > 700 °C the peak of metallic Al (66 eV) increases. Under these conditions Al segregates to the surface and somehow, Al oxide is vanishing, possibly by evaporation of species such as Al_2O, AlO or else. Finally, after > 20 min at about 1000 °C the Al peak decreases and segregation of Cr and S is observed (Figure 3a). The processes observed at the high temperature certainly are very different from the normal oxidation, where Al is selectively oxidized to form a continuous, dense, slow growing Al_2O_3 scale.

Fe–Cr–Al–Y

The general result for the Y-doped samples is that the oxidation of Al is favored in comparison to the undoped specimens and the Al oxide formed is stabilized. The formation of Al oxide and removal of spinels already starts at temperatures slightly above 500 °C, and the oxide stays stable up to about 750 °C (Figure 2b). After longer time at high temperature ~ 1000 °C the oxide vanishes as in the case of the undoped alloy, but it is replaced by segregated Al, not by segregated Cr and S (Figure 3b). Obviously, the yttrium effectively ties up the sulfur in its very stable sulfide and thereby S-segregation is suppressed.

As has already been pointed out, information on surface structures could be obtained by LEED but only after annealing of the samples, which caused Al enrichment by segregation. The oxide formed on such surface does not correspond to bulk Al oxides in any modification, but to surface compounds in the range of a monolayer. The surface oxide grows epitaxially on the (100) and (111) orientations, in the first case a (2×1) overlayer structure is observed (composed of two different domains) and in the second case it is a $(\sqrt{3} \times \sqrt{3})$ R 30°-overlayer structure. On the (110) orientation the growth is not epitaxial and a hexagonal structure with lattice constant 3 Å is observed, but this value does not correspond to α-Al_2O_3.

Morphology and Adherence of the Oxide Scale

The same Fe–Cr–Al alloy and Fe–Cr–Al–Y alloy were also investigated in thermogravimetric oxidation studies at 1000 °C [34]. The oxidation was conducted in a flowing He–O_2 mixture at 100 mbar O_2. Here only the observations on scale morphology and adherence will be reported, which were obtained by scanning electron microscopy.

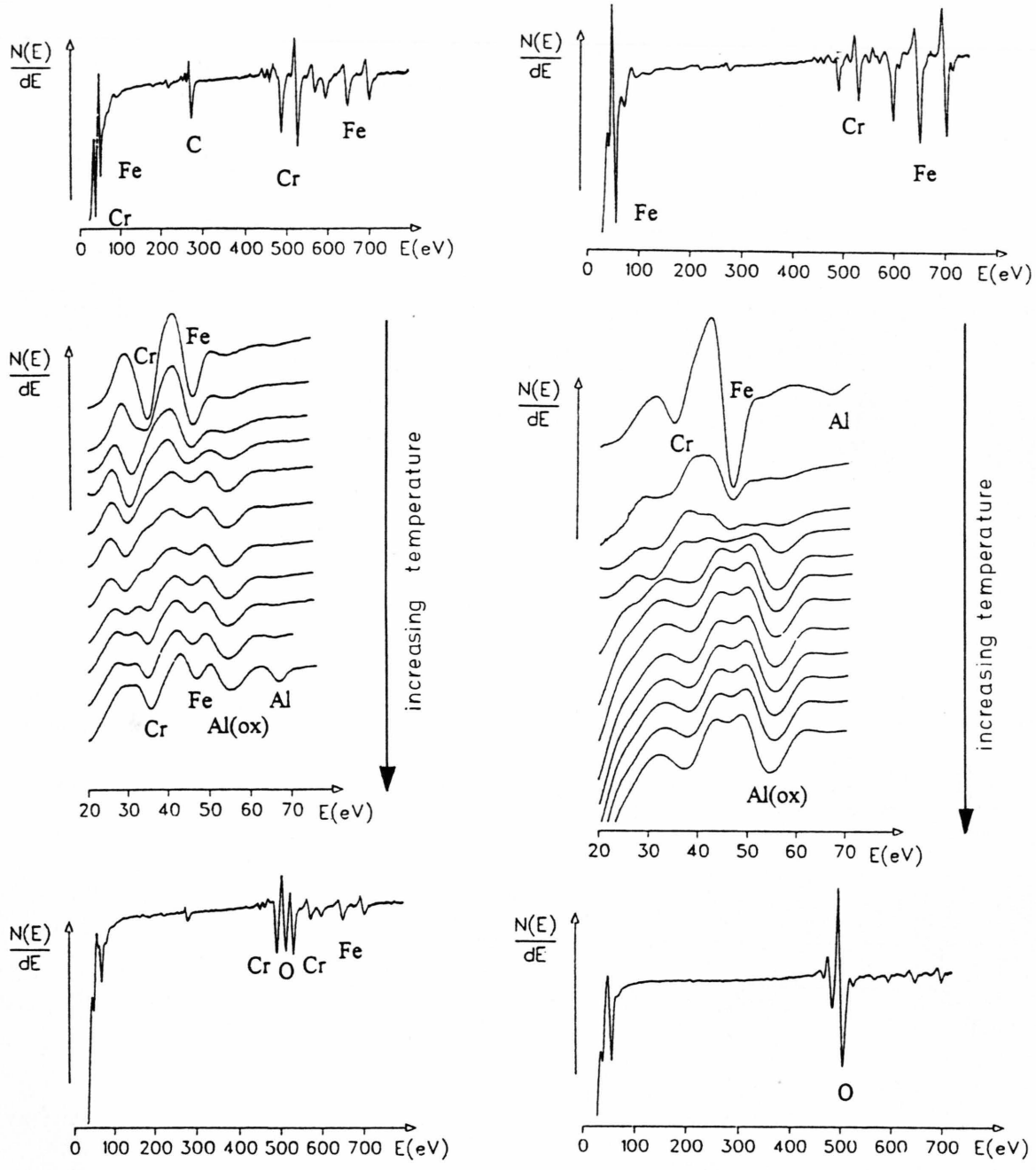

Fig. 2. Auger spectra, taken before and after oxidation at 10^{-7} mbar O_2 up to about 750 °C, and low energy range recorded during oxidation and heating up of the sample. a) (100) surface of Fe–Cr–Al, b) of Fe–Cr–Al–Y (from top to bottom – increasing temperature).

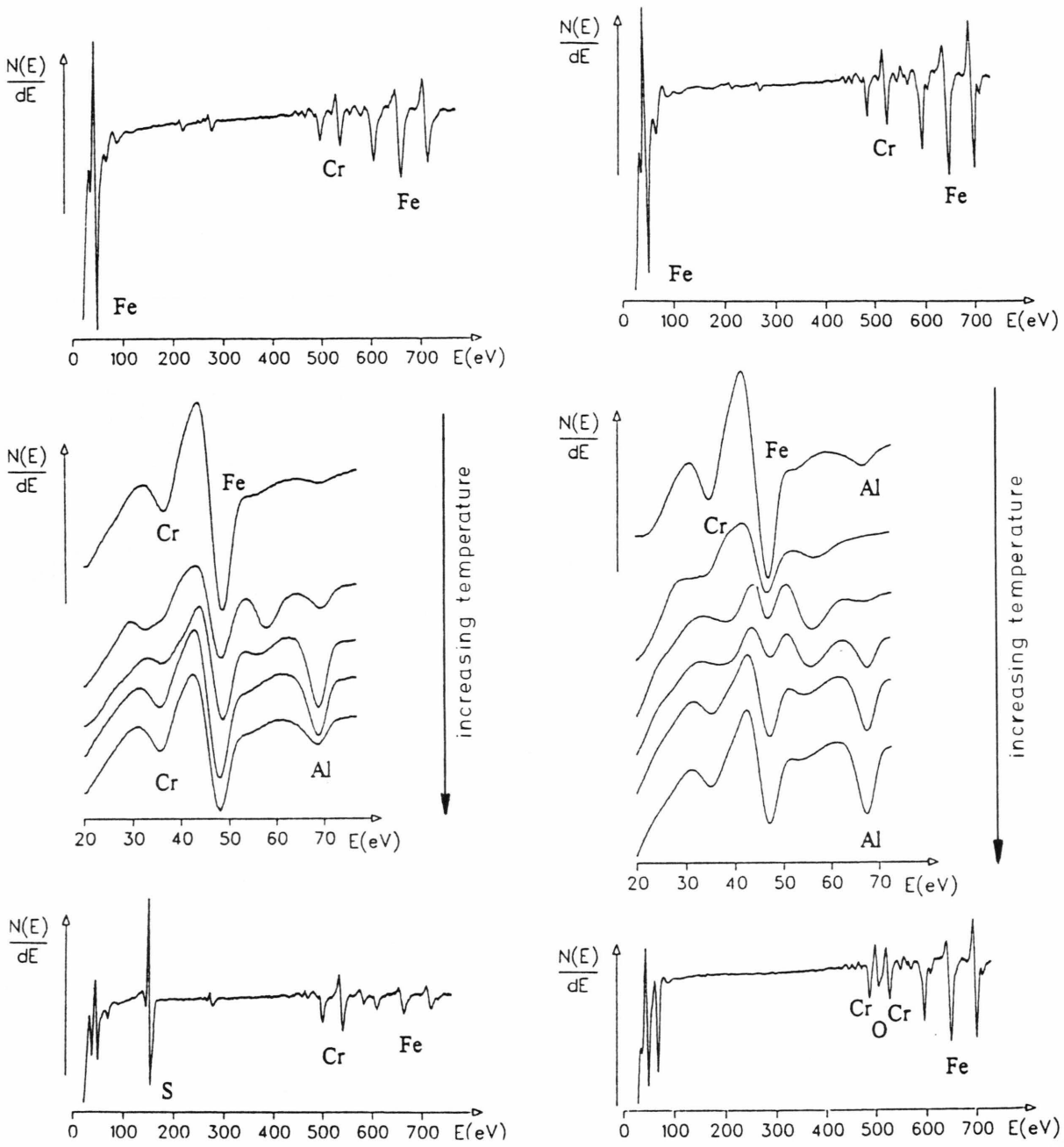

Fig. 3. Auger spectra, taken before and after oxidation at 10^{-7} mbar O_2 up to about 1000 °C, and low energy range recorded during oxidation and heating up of the sample. a) (110) surface of Fe–Cr–Al, b) of Fe–Cr–Al–Y (from top to bottom – increasing temperature).

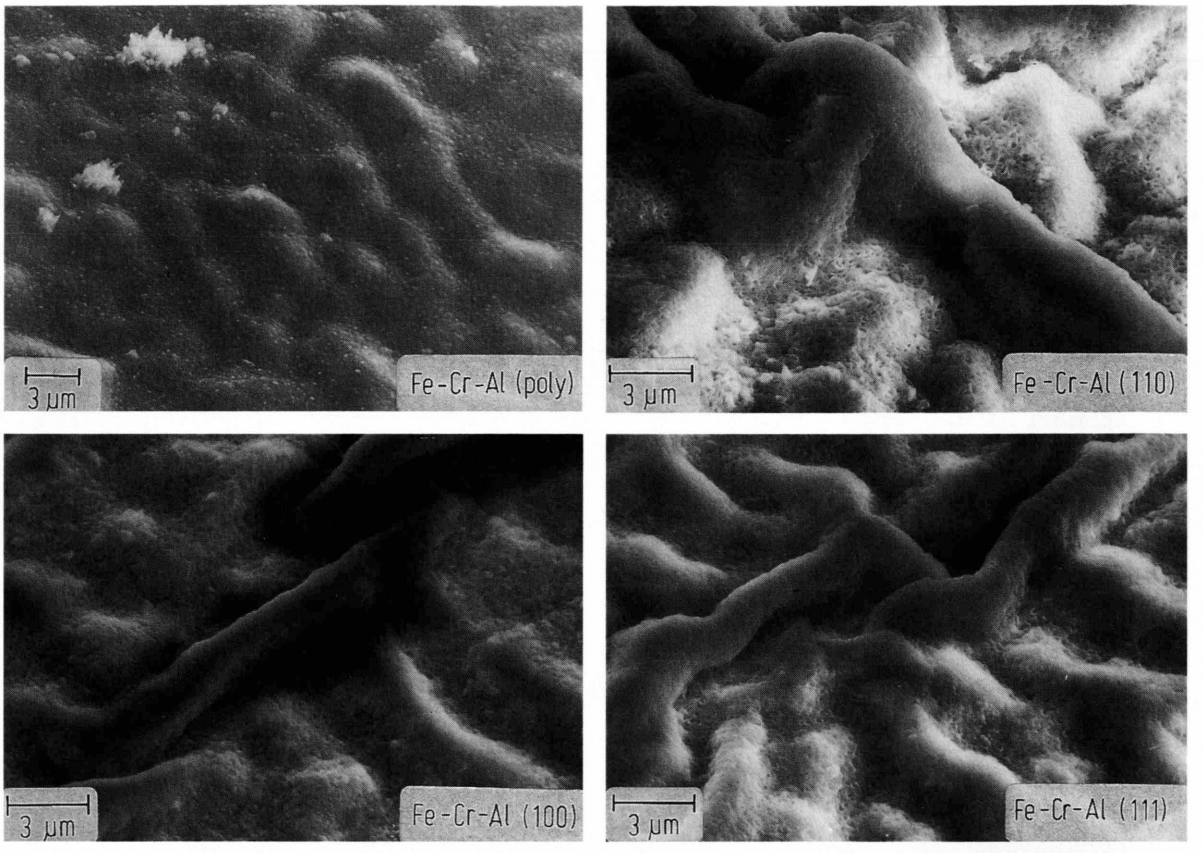

Fig. 4. SEM micrographs showing the surface morphology of the Al_2O_3 scale on Fe–Cr–Al samples after oxidation at 1000 °C and 133 mbar O_2 for 100 h. a) Polycrystalline Fe–Cr–Al, b) Fe–Cr–Al(100), c) Fe–Cr–Al(110), d) Fe–Cr–Al(111).

Fe–Cr–Al

After oxidation of the Fe–Cr–Al alloy at 1000 °C for 100 h a continuous layer of α-Al_2O_3 had formed of about 0.6–0.7 µm thickness. No Cr oxides or Fe oxides were detected and also only traces of other alumina modifications, which stem from the first oxidation stages and are gradually transformed to α-Al_2O_3. After cooling from the oxidation temperature only small areas of oxide remained adherent on the polycrystalline sample, most of the scale spalled, whereas the scale on the single crystal specimens showed better adherence.

The surface morphology after oxidation is shown in Figs. 4a–d for polycrystal and single crystal specimens, on all Y-free specimens the scale is strongly convoluted. These convolutions result from the generally accepted mechanism of lateral growth, by outward diffusion of Al^{3+} cations and inward diffusion of oxygen, mainly at grain boundaries, see Fig. 1a, b. In the case of the polycrystalline alloy the scale remained adherent during scale growth, only a few cavities were formed beneath the scale, see Figure 5a. That means, the substrate is deformed by the growth of the convoluted scale, only in some convex areas (10%) the contact of scale and substrate was lost, leading to the formation of cavities.

The morphology of the scale on the single crystal specimens is very different (Figures 4b–d). The scale forms long convolutions (up to 50 µm) extending along polishing scratches, and short smaller convolutions perpendicular to the first ones. Below the long convolutions the scale has lost contact with the substrate and long extending cavities are detected here (Figures 5b–d). After short oxidation (5 h) there are only a few cavities at the scale/alloy interface on the

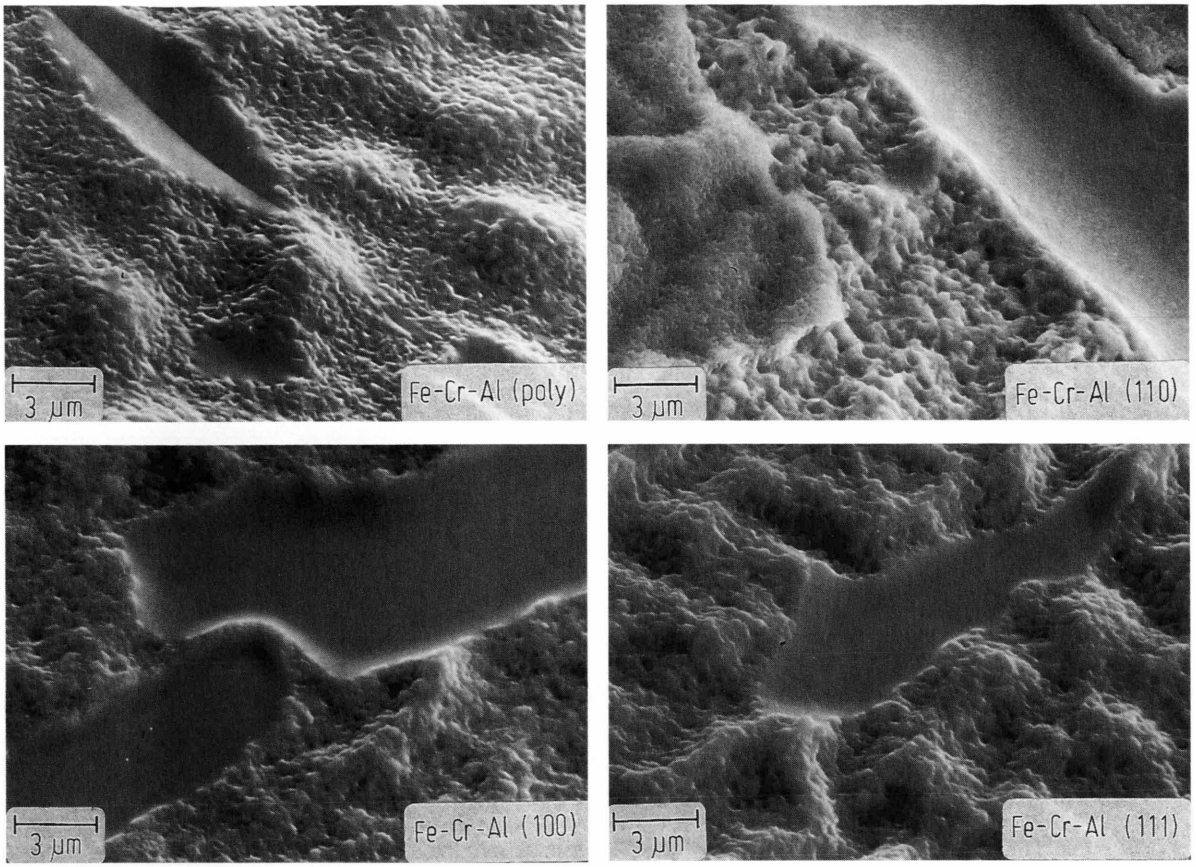

Fig. 5. SEM micrographs showing the surface morphology of the same specimens as in Fig. 5 but after complete or partial detachment of the scale – imprinted areas had been in contact with the scale, smooth areas are the metal surfaces below cavities. a) Polycrystalline Fe–Cr–Al, b) Fe–Cr–Al(100), c) Fe–Cr–Al(110), d) Fe–Cr–Al(111).

(110) sample and almost no cavities on samples of other orientations. The difference of the scale morphologies on polycrystal and single crystal specimens is not caused by the grain boundaries, since the grain size of the polycrystalline sample was 0.5 mm and the influence of the grain boundaries on the scale growth was negligible. Thus, the observed difference appears to be only related to the surface orientations of the samples. Since the α-Al_2O_3 is not epitaxial with the bcc lattice, the differences must be explained by the interfacial energies on the three orientations studied. Generally the scale curvature, size and number of cavities are higher on the (100) and (110) surfaces, which have the lower surface energies, than on the (111) surface which has a high surface energy. The metal surfaces with the low surface energy are very stable and do not follow the undulated oxide layer, but separate under cavity formation. The (111) surface is more disposed to change the orientation, staying adherent to the oxide layer and deforming with its growth, and the randomly oriented surface on the polycrystalline specimen changes its structure even easier. The bottom of the cavities on the (100) surface is very flat and parallel to the whole surface, i.e. it keeps the (100) orientation (Figure 5 b). Probably, this orientation is stabilized after the separation by surface segregation of impurities, mainly sulfur [20]. In contrast, the bottom of cavities on the (110) surface is semi-elliptically shaped in section, most probably due to segregation and surface reconstruction after the segregation. In cavities on the (111) surface, facetting is observed which is to be expected because of its high surface energy and low stability.

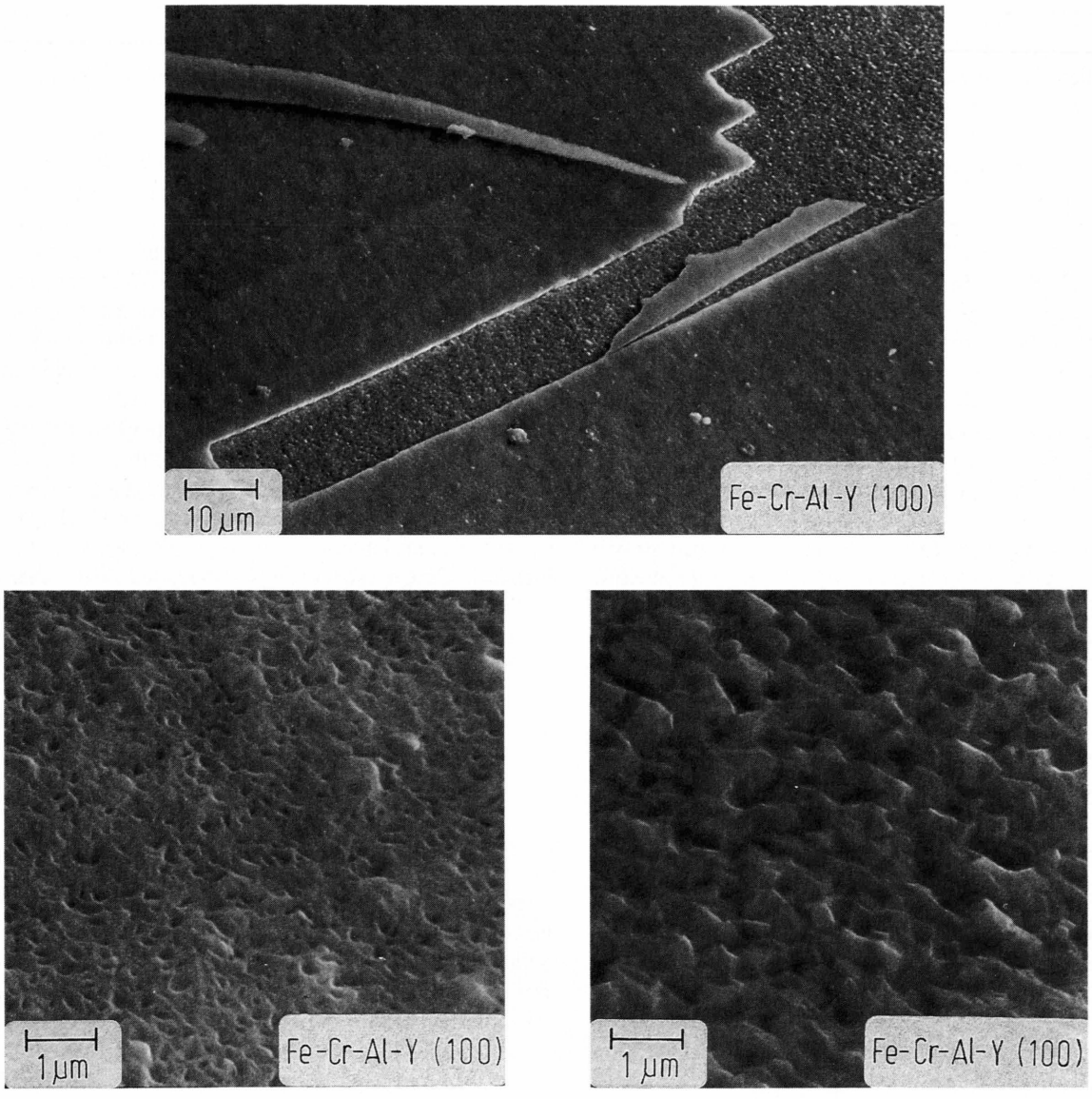

Fig. 6. SEM micrographs showing the surface morphology of Fe–Cr–Al–Y (100) after oxidation at 1000 °C and 133 mbar O_2 for 100 h, and after bending the specimen to cause spalling of the scale. a) Overview, scale partially spalled, b) high magnification micrographs at the scale surface and c) of the metal substrate surface (detached area).

Upon cooling, the scale spalls more or less from wide areas of all undoped Fe–Cr–Al specimens, because of the different contraction of scale and substrate. For an uneven interface thermal stresses occur, which can be tangential but also normal to the interface with maxima of tensile stress at the top of convex areas [35]. These stresses are the main reason for scale spallation during cooling of the yttrium-free alloy.

Fe–Cr–Al–Y

The distinct difference in the morphologies of the oxide scale on the Fe–Cr–Al and the Fe–Cr–Al–Y alloys is that the oxide scale on the latter is almost perfectly flat (Fig. 6 a and b). This is observed independent of the surface orientation. Bending of the oxidized Fe–Cr–Al–Y samples reveals the metal surface

under the spalled scale. This surface is also flat and shows small imprints of oxide grains (Fig. 6c), but no cavities. The structure of the scale is similar as on the undoped Fe–Cr–Al alloys, concerning grain size and thickness. The absence of scale convolutions and of cavities beneath the scale can be explained only by the assumption that yttrium suppresses the lateral growth, nearly no growth stresses are developed and there is no cause for the formation of scale convolutions. This assumption is supported by marker experiments and experiments with oxygen isotopes [10] which indicate that in the presence of Y the Al_2O_3 scale grows only by inward diffusion of oxygen. The suppression of cation diffusion in the scale eliminates lateral growth and results in a flat scale configuration. If the cavity formation at the scale/alloy interface is the result of scale convolution, it is evident that under the flat oxide layer there are no voids or cavities.

The adherence of the scale on the Y-doped alloy is excellent, even repeated thermal cycling did not cause spallation. The thermal stresses resulting from the different contraction and expansion of scale and alloy do not lead to cracking, buckling or separation, the stresses are homogeneously distributed parallel to the flat interface. After cooling the stress state of the oxide scale is uniform biaxial compression, there are no stresses normal to the interface and no shear stresses at the interface [35], thus there is no reason for scale separation.

Conclusions

Studies on the initial stages of oxidation were conducted at low $pO_2 \sim 10^{-7}$ mbar up to 1000 °C, following the changes on the surfaces by AES. Some observations are well in agreement with what is known from studies at high pressures, i.e. the initial formation of (Fe, Cr) oxides at intermediate temperature $\sim$ 500 °C which are displaced at higher temperature by Al oxide. The Al oxide, however, vanishes at higher temperature $>$ 900 °C, due to further Al segregation and insufficient oxygen supply for its oxidation, at higher pO_2 a stable α-Al_2O_3 layer would be formed.

The doping with yttrium somehow fostered the formation of Al oxide already at intermediate temperature and stabilized it up to high temperature. In contrast to the undoped alloy no sulfur segregation occurred after extended exposure at the high temperature, obviously the sulfur is strongly bound in Y-sulfide precipitates.

It must be emphasized that the Al-oxide observed is no bulk compound, but consists of only a few layers. The LEED studies showed that these surface compounds have no direct relation to bulk Al-oxides.

Concerning the RE effect, none of the mechanisms described has been clearly confirmed. Certainly, the presence of yttrium favored the Al-oxide formation and stabilized it. Only the mechanism 1. the action of yttrium or yttrium oxides as nucleation sites may play a role in the phenomena observed. However, no enrichment of Y at the surface was detected by AES, the concentration necessary for improving the Al_2O_3 nucleation must be very low ($< 1\%$ coverage). The latter observation also rules out mechanisms, for which considerable Y-enrichments would be necessary at the interface, i.e. the mechanisms 2. "Graded Seal" layer, 8. Enhanced chemical bonding and 10. Blocking of interface.

The SEM studies of oxide morphologies clearly indicate that there must be a change in growth processes (mechanism 3) caused by the presence of yttrium. On Fe–Cr–Al very convoluted scales are observed, which tend to spall upon cooling. In Fe–Cr–Al–Y the scales are flat and well adherent, which is explained by the suppression of counterdiffusion of oxygen and cations due to yttrium enrichment at the oxide grain boundaries [9–12]. A new result was obtained by the use of Fe–Cr–Al single crystals: The separation of oxide and scale is clearly dependent on the surface energy of the metal surface to be formed. Distinctly more cavity formation was observed on the single crystals with the main orientations (110) and (100) where these low energy surfaces have to be formed, than on the specimen with (111) orientation and on the polycrystalline Fe–Cr–Al.

Acknowledgement

Support of this study by the Deutsche Forschungsgemeinschaft is gratefully acknowledged. V. K. Tolpygo thanks the Max-Planck-Gesellschaft for supporting his stay as a guest scientist at the Max-Planck-Institut für Eisenforschung.

[1] D. P. Whittle and J. Stringer, Phil. Trans. Roy. Soc. London **A 259,** 309 (1980).
[2] J. Stringer, Mat. Sci. Engg. **A 120,** 129 (1989).
[3] D. P. Moon, Mater. Sci. Techn. **5,** 754 (1989).
[4] D. P. Moon and M. J. Bennett, Mat. Sci. Forum **43,** 269 (1989).
[5] J. Jedlinski, Solid State Phenomena **21/22,** 335 (1992).
[6] T. N. Rhys-Jones, H. J. Grabke, and H. Kudielka, Corros. Sci. **27,** 49 (1987).
[7] J. Peters and H. J. Grabke, Werkstoffe u. Korr. **35,** 385 (1984).
[8] J. Peters, H. J. Grabke, and H. Viefhaus, Proc. 10th Symp. Reactivity of Solids, Dijon, Eds. P. Barret and L. C. Dufour, Elsevier 1985, p. 151–156.
[9] F. A. Golightly, F. H. Stott, and G. C. Wood, Oxid. Met. **10,** 163 (1976); **14,** 218 (1980).
[10] W. J. Quadakkers, H. Holzbrecher, K. G. Briefs, and H. Beske, Oxid. Met. **32,** 67 (1989).
[11] J. Jedlinski and S. Mrowec, Mater. Sci. Engg. **87,** 281 (1987).
[12] S. Mrowec and J. Jedlinski, Trans. TMS AIME **247,** 1099 (1988).
[13] A. W. Funkenbusch, J. G. Smeggil, and N. S. Bornstein, Metall. Trans. **16 A,** 1164 (1985).
[14] J. G. Smeggil, A. W. Funkenbusch, and N. S. Bornstein, Metall. Trans. **17 A,** 923 (1986).
[15] J. G. Smeggil, N. S. Bornstein, and M. A. DeCrescente, Oxid. Met. **30,** 259 (1988).
[16] J. L. Smialek, Metall. Trans. **18 A,** 164 (1987).
[17] D. R. Sigler, Oxid. Metals **29,** 23 (1988).
[18] H. J. Grabke, D. Wiemer, and H. Viefhaus, Appl. Surf. Sci. **47,** 243 (1991).
[19] H. J. Grabke, G. Kurbatov, and H. J. Schmutzler, Oxid. Met., in press.
[20] H. J. Schmutzler, H. Viefhaus, and H. J. Grabke, Surf. Interface Anal. **18,** 581 (1992).
[21] I. M. Allam, D. P. Whittle, and J. Stringer, Oxid. Met. **12,** 35 (1978); **13,** 35 (1979).
[22] T. A. Ramanarayanan, R. Ayer, R. Petkovic-Luton, and D. P. Leta, Oxid. Met. **29,** 445 (1988).
[23] J. K. Tien and F. S. Pettit, Metall. Trans. **3,** 1587 (1972).
[24] J. D. Kuenzly and D. L. Douglass, Oxid. Metals **8,** 139 (1974).
[25] J. C. Pivin, D. Delaunay, C. Roques-Carmes, A. M. Huntz, and P. Lacombe, Corros. Sci. **20,** 351 (1981).
[26] A. B. Anderson, S. P. Mehandru, and J. Smialek, J. Electrochem. Soc. **132,** 1695 (1985).
[27] D. Delaunay and A. M. Huntz, J. Mat. Sci. **17,** 2027 (1982).
[28] H. Hindam and D. P. Whittle, Oxid. Metals **18,** 245 (1982).
[29] B. Pieraggi and R. A. Rapp, J. de Physique IV, Colloque C9, Supplément au J. de Physique III, Vol. **3,** 275 (1993).
[30] R. A. Rapp, "Adhesion of Oxide Scales" in Mat. Sci. Forum Vol. 154 "Surface Layers", Eds. M. A. J. Somers, E. J. Mittemeijer, and J. Schoonman, Trans. Tech. Publ. Switzerland 1994, pp. 119–128.
[31] M. Siegers, H. J. Grabke, and H. Viefhaus, in "Microscopy of Oxidation 2", Ed. S. B. Newcomb and M. J. Bennett, The Inst. of Materials, London 1993, p. 269.
[32] M. Siegers, H. J. Grabke, and H. Viefhaus, Fresenius J. Anal. Chem. **346,** 269 (1993).
[33] M. Siegers, H. J. Grabke, and H. Viefhaus, in "Progress in Understanding and Protection of Corrosion" (Proceed. EUROCORR '93), Ed. J. M. Costa and A. D. Mercer. The Inst. of Materials, London 1993, p. 777.
[34] V. K. Tolpygo and H. J. Grabke, Oxid. Met. **41,** 343 (1994).
[35] A. G. Evans, G. B. Crumley, and R. E. Demaray, Oxid. Met. **20,** 193 (1983).